Quantum state preparation and nonunitary evolution with diagonal operators

Anthony W. Schlimgen,[1] Kade Head-Marsden,[2] LeeAnn M. Sager-Smith,[1]
Prineha Narang,[2] and David A. Mazziotti[1,*]

[1]*Department of Chemistry and The James Franck Institute, The University of Chicago, Chicago, Illinois 60637, USA*
[2]*John A. Paulson School of Engineering and Applied Sciences, Harvard University, Cambridge, Massachusetts 02138, USA*

(Received 6 May 2022; accepted 2 August 2022; published 16 August 2022)

Realizing nonunitary transformations on unitary-gate-based quantum devices is critically important for simulating a variety of physical problems, including open quantum systems and subnormalized quantum states. We present a dilation-based algorithm to simulate nonunitary operations using probabilistic quantum computing with only one ancilla qubit. We utilize the singular-value decomposition (SVD) to decompose any general quantum operator into a product of two unitary operators and a diagonal nonunitary operator, which we show can be implemented by a diagonal unitary operator in a one-qubit dilated space. While dilation techniques increase the number of qubits in the calculation, and thus the gate complexity, our algorithm limits the operations required in the dilated space to a diagonal unitary operator, which has known circuit decompositions. We use this algorithm to prepare random subnormalized two-level states on a quantum device with high fidelity. Furthermore, we present the accurate nonunitary dynamics of two-level open quantum systems in a dephasing channel and an amplitude-damping channel computed on a quantum device. The algorithm presented will be most useful for implementing general nonunitary operations when the SVD can be readily computed, which is the case for most operators in the noisy intermediate-scale quantum computing era.

DOI: 10.1103/PhysRevA.106.022414

I. INTRODUCTION

Recent advances in quantum computation have enabled algorithm implementation on real quantum devices in the noisy intermediate-scale quantum (NISQ) regime [1]. This regime is defined by low-qubit counts where decoherence times are relatively short and two-qubit gate errors remain problematic. The noise experienced by the device presents a challenge towards practical algorithm implementation that has led to a plethora of research across chemistry, physics, and engineering [2–7]. One area that has been gaining recent attention is algorithm development for the nonunitary time evolution of quantum systems. Current quantum devices are typically unitary gate based, so nonunitary operators must be cast as unitary in order to be practically implementable. There are a variety of algorithms which have been developed to bypass this obstacle, including explicit mathematical dilations [8–15], quantum imaginary time evolution [16], duality [17,18], the variational principle [19], collision models [20], analog simulation [21], and others [22–33]. The majority of these algorithms rely on some form of dilation, either mapping the operator to a larger Hilbert space or adding ancilla qubits. Another way to view this problem is through the lens of non-normalized state preparation. Nonunitary operations are not norm conserving, so evolution of a state nonunitarily will result in a subnormalized state.

Here, we present and demonstrate a dilation-based algorithm using nonunitary diagonal operators. Diagonal operators are relatively sparse and have known circuit decompositions, which make them attractive for multiqubit calculations. We show that nonunitary diagonals can be transformed to unitary diagonals with a one-qubit dilation. The algorithm is probabilistic, but the success probability of preparing the desired state can be improved with standard amplitude-amplification techniques because the desired state is known. Finally, the exact preparation of the desired state requires $O(2^{k+1})$ one- and two-qubit gates, where k is the number of system qubits. Importantly, diagonal gates can also be implemented approximately with controlled error, requiring only a polynomial number of gates with respect to the number of qubits [34].

This dilation can be used for probabilistic state preparation as well as nonunitary evolution of quantum states. Dilated diagonals can be utilized to prepare both normalized and subnormalized states. While subnormalized states can always be normalized before a quantum simulation, the situation often arises where the state needs to be manipulated further on a quantum device in its subnormalized form as, for example, in preparing linear combinations with other un-normalized states. In this work, we prepare a random selection of subnormalized states on an IBM quantum device and perform a tomography of those states, demonstrating that we can achieve high-fidelity state preparation.

Subnormalized states also arise in the context of nonunitary dynamics. Using the singular-value decomposition (SVD), we show that any nonunitary operator can be written in terms of two unitaries and a nonunitary diagonal operator, which can be dilated to a unitary. The classical cost of the algorithm is the cost of the SVD, which scales as $O(r^3)$, where r is the size of the original operator. It is worth noting that this is the most general case and does not preclude the possibility of reduced

*damazz@uchicago.edu

classical scaling in special cases. Our algorithm requires only one ancilla qubit for any size operator, and the entangling operations between the state and ancilla are reduced to a diagonal gate, which is efficient to implement. In the limit of a large number of qubits, our dilated algorithm is approximately double the cost of a unitary propagation on the original Hilbert space in terms of circuit depth. On the other hand, compared to a general dilated unitary operator, our algorithm reduces the circuit depth by approximately half.

We outline the nonunitary diagonal operator implementation for state preparation in Sec. II A and the SVD algorithm for nonunitary evolution in Sec. II B. The computational methodology is laid out in Sec. III, then demonstrated on the preparation of subnormalized states and open-system dynamics in Secs. IV A and IV B, respectively.

II. THEORY

A. Nonunitary diagonal operators and quantum state preparation

Due to their sparsity, diagonal operators are attractive transformations for quantum simulation, and there are known algorithms for efficient implementation of unitary diagonals [34,35]. Here, we show that nonunitary diagonals can be implemented as unitary diagonal gates with only one ancilla qubit. Consider a nonunitary diagonal operator $\hat{\Sigma}$ with complex entries σ_{jj} on the diagonal, and assume the magnitude of each element is less than or equal to unity. We can directly construct a unitary diagonal operator,

$$\hat{U}_{\hat{\Sigma}} = \begin{pmatrix} \hat{\Sigma}_+ & 0 \\ 0 & \hat{\Sigma}_- \end{pmatrix}, \tag{1}$$

where

$$\hat{\Sigma}_{jj\pm} = \sigma_{jj} \pm i\sqrt{\frac{1-||\sigma_{jj}||^2}{||\sigma_{jj}||^2}}\sigma_{jj}. \tag{2}$$

We also write Eq. (1) as $\hat{U}_{\hat{\Sigma}} = \hat{\Sigma}_+ \oplus \hat{\Sigma}_-$, where $\oplus$ is the block, or direct sum operator. We emphasize that $2\hat{\Sigma} = \hat{\Sigma}_+ + \hat{\Sigma}_-$. If the size of the nonunitary diagonal operator is r, then the size of the dilated unitary $\hat{U}_{\hat{\Sigma}}$ is $2r$. This implies that the dilated unitary can be implemented on a quantum device with only one ancilla qubit because we only need to double the size of the original Hilbert space. Importantly, the dilated unitary is trivial to compute from the nonunitary diagonal, requires no matrix operations to generate the unitary, and requires no recursive decomposition to compute rotation angles.

We can achieve the probabilistic application of the nonunitary diagonal operator by preparing the ancilla qubit in the superposed state and recombining the states after application of $\hat{U}_{\hat{\Sigma}}$, as shown in Fig. 1. The algorithm is successful when the ancilla qubit is in state $|0\rangle$, and the nonunitary $\hat{\Sigma}$ is applied to state $|\psi\rangle$. The desired state is known, so the success probability can be increased with standard techniques of amplitude amplification [36–39].

We show how to use this technique to prepare a known quantum state,

$$|\phi\rangle = \sum_j c_j|j\rangle. \tag{3}$$

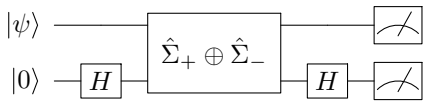

FIG. 1. Circuit for implementing a nonunitary diagonal operator $\hat{\Sigma}$ on $|\psi\rangle$ using only unitary gates with a one-qubit dilation. The final gate on each rail is the measurement gate, H is the Hadamard gate, and the multiqubit gate is the diagonal operator in Eq. (1). The algorithm is successful when the ancilla is measured in state $|0\rangle$.

First, generate the superposition of quantum states on $k+1$ qubits, then apply $\hat{U}_{\hat{\Sigma}}$, and last, perform linear combinations of $\hat{\Sigma}_\pm$ applied to the superposed state. We can generate the desired unitary $\hat{U}_{\hat{\Sigma}}$ by defining the diagonal operator $\hat{\Sigma}$ with elements, $\hat{\Sigma}_{jj} = c_j$. The amplitudes of the desired state are encoded in the dilated Hilbert space and generated with the transformation

$$|\Psi\rangle = (I^{\otimes k} \otimes H)\hat{U}_{\hat{\Sigma}}(H^{\otimes k}|0\rangle^{\otimes k} \otimes H|0\rangle). \tag{4}$$

The desired state $|\phi\rangle$ is encoded probabilistically in the dilated space as

$$|\Psi\rangle = \frac{1}{2^{\frac{k}{2}+1}}\begin{pmatrix} (\hat{\Sigma}_+ + \hat{\Sigma}_-)|\tilde{k}\rangle \\ (\hat{\Sigma}_+ - \hat{\Sigma}_-)|\tilde{k}\rangle \end{pmatrix}, \tag{5}$$

where $|\tilde{k}\rangle$ indicates the superposed state on k qubits. When the ancilla qubit is in state $|0\rangle$ a state proportional to $|\phi\rangle$ is prepared, as desired. When the ancilla qubit is in state $|1\rangle$, the algorithm does not prepare the desired state, and the resulting state is not of interest. This has some similarity to standard state-initialization techniques in that both utilize a diagonal operator. Standard techniques, however, compute the unitary required to take the ground state to the desired state. Instead, we take the superposed state to the desired state probabilistically, through a nonunitary transformation with an ancilla qubit.

This approach can be used for preparation of subnormalized states as well as normalized states. An ensemble state is characterized by a positive sum of density matrices,

$$\rho = \sum_i p_i\rho_i. \tag{6}$$

While each ρ_i is a pure state and can be individually normalized, it can be useful to prepare the subnormalized states $p_i\rho_i$, which can be further transformed on a quantum device. Probabilistic normalized state preparation in this form is thus more expensive in terms of gate depth compared to standard state-initialization techniques due to the ancilla qubit and larger diagonal operator. In contrast, the computation of the diagonal operator needed for this state preparation is immediately available from the simple arithmetic in Eq. (2) and requires no recursive decomposition. Furthermore, our probabilistic approach allows for the preparation of non-normalized states and therefore the implementation of nonunitary operators. We discuss the circuit complexity for diagonal operators in the next section.

B. Nonunitary evolution

A quantum system represented by a density matrix ρ undergoing nonunitary evolution can be characterized by unitary

evolution in a dilated Hilbert space, where the state is coupled to some environment σ_B. This can be expressed with Stinespring's dilation, where the propagated density matrix $\rho(t)$ is given by the partial trace of the unitary evolution of the interacting system and environment [9,40–42].

A more cost-effective method is the Sz.-Nagy dilation, which was originally applied to contraction mappings and requires only one ancilla qubit for implementation [10,12]. The one-dilation for a nonunitary operator $\hat{M}$ can be written as

$$\hat{U}_{\hat{M}} = \begin{pmatrix} \hat{M} & \sqrt{I - \hat{M}\hat{M}^\dagger} \\ \sqrt{I - \hat{M}^\dagger\hat{M}} & -\hat{M}^\dagger \end{pmatrix}, \tag{7}$$

where the off-diagonal elements are known as the defect operators. The dilation is guaranteed when $\hat{M}$ is a contraction, so the square root in the defect operator is defined, and any bounded operator can be shifted to a contraction [10]. While this dilation requires only one ancilla qubit, the dilated unitary acts over the entire dilated space, which can lead to quantum circuits with high gate counts when the system becomes large.

Consider instead the SVD for $\hat{M}$,

$$\hat{M} = \hat{U}\hat{\Sigma}\hat{V}^\dagger, \tag{8}$$

where $\hat{U}$ and $\hat{V}^\dagger$ are unitary operators and $\hat{\Sigma}$ is a diagonal operator of the singular values of $\hat{M}$, which are always real and non-negative. Since $\hat{U}$ and $\hat{V}^\dagger$ are unitary, they can be implemented on a space that is the same size as the original operator $\hat{M}$, but $\hat{\Sigma}$ is nonunitary and must be dilated, as shown above. The SVD has been used to analyze nonunitary operations in other quantum algorithms [43,44]; however, we show here that the singular-value matrix can be implemented efficiently as a diagonal operator and is the only operator that must span the dilated space. Importantly, the implementation of the nonunitary operation here does not depend on an expansion parameter as in other works [14,43,44], so the operation can be implemented exactly, as long as decompositions for U and $V^\dagger$ can be performed.

The formulation of the singular values in Eq. (2) is inspired by the Sz.-Nagy dilation in Eq. (7), where the square-root term is reminiscent of the defect operator. Indeed, the unitary in Eq. (1) is related to the standard form of the Sz.-Nagy dilation by a rotation; however, the present formulation maintains the diagonal structure of the singular-value matrix, which generally results in shallower circuits.

While the singular values are always real and non-negative, Eq. (2) is suitable for any real or complex number as long as its magnitude is bound by 1. In the case of singular values of magnitude greater than 1, simply dividing $\hat{\Sigma}$ by the largest singular value will ensure that Eq. (1) remains unitary. In fact, dividing by the largest singular value results in an operator that is always a contraction, which guarantees a Sz.-Nagy dilation. This observation is related to that of Hu *et al.*, who showed that since every bounded operator is bounded by its Hilbert-Schmidt norm, it can be shifted to an operator that is always a contraction [10]. Shifting the operator, or scaling it by the largest singular value, will affect the success probability of the algorithm, but the success probability can be driven towards unity with amplitude amplification.

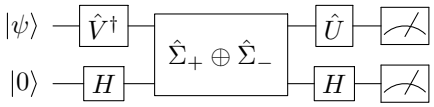

FIG. 2. Circuit for implementing the nonunitary operator $\hat{M}$ on $|\psi\rangle$ using only unitary gates with a one-qubit dilation. The final gate on each rail is the measurement gate, and all other gates are defined in the text. The only operator acting over the dilated space is the diagonal operator, and the linear combinations are performed using the Hadamard gates.

Generating the singular values requires computing the sum of $\hat{\Sigma}_+$ and $\hat{\Sigma}_-$. Linear combinations of unitary operators are, in general, nonunitary; however, we can implement linear combinations of unitary operators using the block-sum, or direct-sum, approach, as in Eq. (1). The nonunitary propagation of $|\psi\rangle$, including the linear combinations, can be performed with the following transformation:

$$\begin{aligned} &\frac{1}{2}\begin{pmatrix} I & I \\ I & -I \end{pmatrix}\begin{pmatrix} \hat{U} & 0 \\ 0 & \hat{U} \end{pmatrix}\begin{pmatrix} \hat{\Sigma}_+ & 0 \\ 0 & \hat{\Sigma}_- \end{pmatrix}\begin{pmatrix} \hat{V}^\dagger & 0 \\ 0 & \hat{V}^\dagger \end{pmatrix}\begin{pmatrix} |\psi\rangle \\ |\psi\rangle \end{pmatrix} \\ &\quad = \frac{1}{2}\begin{pmatrix} \hat{U}(\hat{\Sigma}_+ + \hat{\Sigma}_-)\hat{V}^\dagger|\psi\rangle \\ \hat{U}(\hat{\Sigma}_+ - \hat{\Sigma}_-)\hat{V}^\dagger|\psi\rangle \end{pmatrix} = \begin{pmatrix} \hat{M}|\psi\rangle \\ \hat{M}^-|\psi\rangle \end{pmatrix}, \end{aligned} \tag{9}$$

where we note that $\hat{M} = \frac{1}{2}\hat{U}(\hat{\Sigma}_+ + \hat{\Sigma}_-)\hat{V}^\dagger$ and define $\hat{M}^- = \frac{1}{2}\hat{U}(\hat{\Sigma}_+ - \hat{\Sigma}_-)\hat{V}^\dagger$. We again note that we discard the states corresponding to $\hat{M}^-|\psi\rangle$. The linear combinations are achieved through the final Hadamard gate on the ancilla qubit, as discussed elsewhere [14,45–47]. Finally, while we have shown this transformation for a pure state, using the eigendecomposition of a mixed state along with linearity allows for the straightforward application of Eq. (9) to mixed states. We show in the next section that, after assuming the classical cost of the SVD, the decomposition in Eq. (9) can be implemented on a quantum circuit, with minimal operations spanning the entire dilated space. The SVD is typically computed with a bidiagonalization and QR decomposition approach, with a classical cost of $O(r^3)$, where r is the size of the operator. Due to the special structure of the operators in this work, their SVDs are available by inspection, so numerical decomposition is not necessary in these cases.

III. METHODS

We show the general circuit for implementing Eq. (9) in Fig. 2. The nonunitary propagation of a quantum state in an r-dimensional Hilbert space can be implemented on a quantum circuit with $k+1$ qubits, where $k \geqslant \log_2(r)$. This circuit requires the implementation of two k-qubit operators, $\hat{V}^\dagger$ and $\hat{U}$, along with a $(k+1)$-qubit diagonal operator, $\hat{U}_{\hat{\Sigma}} = \hat{\Sigma}_+ \oplus \hat{\Sigma}_-$. The following identities are useful to derive Eq. (9):

$$\begin{aligned} \hat{U} \otimes I &= \begin{pmatrix} \hat{U} & 0 \\ 0 & \hat{U} \end{pmatrix}, \\ I \otimes H &= \frac{1}{\sqrt{2}}\begin{pmatrix} I & I \\ I & -I \end{pmatrix}, \\ (I \otimes H)(|\psi\rangle \otimes |0\rangle) &= \frac{1}{\sqrt{2}}\begin{pmatrix} |\psi\rangle \\ |\psi\rangle \end{pmatrix}. \end{aligned} \tag{10}$$

This formulation leads to a reduction in algorithm complexity because the only operator to act on the larger one-dilated space is a diagonal operator, which is, in general, less expensive to implement compared to a dense one-dilated operator.

To see this reduction in cost, let the dilated space require $d = k + 1$ qubits, and consider a general unitary that can be decomposed into $O(d^2 2^{2d})$ one-qubit and controlled NOT (CNOT) gates [42]. The diagonal gate operating over d qubits can be exactly decomposed into at most $2^{d+1} - 3$ fundamental gates [48], and the operators $\hat{U}$ and $\hat{V}^\dagger$ can each be implemented with $O([d-1]^2 2^{2d-2})$ gates. To leading order, therefore, our algorithm reduces the circuit depth by factor of 2, resulting in a complexity of $O(d^2 2^{2d-1})$ compared to the dense d-qubit operator.

As d becomes large, the cost of our algorithm is dominated by the implementation of the unitaries $\hat{U}$ and $\hat{V}^\dagger$, and the cost of the dilated diagonal operator becomes negligible. Seen in this way, our algorithm to implement a k-qubit nonunitary operator is twice as expensive as a k-qubit unitary operator in the large-k limit. The exact implementation of diagonal gates results in the gate counts above; however, approximate polynomial implementations of diagonal gates are also known [34]. If U and $V^\dagger$ are k-local operators, then the exponential scaling of the method can be avoided if the diagonal operator is also implemented approximately [49].

IV. RESULTS

A. Preparation of subnormalized states

Here, we show the algorithm's utility in preparing known subnormalized quantum states on quantum devices. Using a PYTHON seeded random-number generator, we pseudorandomly generated 98 complex subnormalized one-qubit states $|\psi_1\rangle$ from normalized two-qubit states $|\psi_2\rangle$,

$$\begin{aligned} |\psi_2\rangle &= a_{00}|00\rangle + a_{01}|01\rangle + a_{10}|10\rangle + a_{11}|11\rangle, \\ |\psi_1\rangle &= a_{00}|0\rangle + a_{01}|1\rangle. \end{aligned} \tag{11}$$

State $|\psi_1\rangle$ is then prepared probabilistically using the circuit in Fig. 1 and Eq. (2), i.e.,

$$\hat{\Sigma} = \begin{pmatrix} a_{00} & 0 \\ 0 & a_{01} \end{pmatrix}. \tag{12}$$

The average norm of states $|\psi_1\rangle$ is 0.67 ± 0.12.

For each state we prepared a two-qubit circuit, initializing each qubit with a Hadamard gate, followed by implementing the diagonal operator in Eq. (2), using the diagonal operator decomposition available in QISKIT [48,50]. We perform full tomography of state $|\psi_1\rangle\langle\psi_1|$, which requires three circuits, then compute the fidelity and distance between the exact classical state ρ_E and the state from device tomography ρ_S [42]. The fidelity is given by

$$F(\rho_S, \rho_E) = \mathrm{Tr}\left(\sqrt{\sqrt{\rho_S}\rho_E\sqrt{\rho_S}}\right)^2, \tag{13}$$

and the distance is the Frobenius norm of the difference of the exact and simulated density matrices. The distance is computed between the un-normalized states, while the fidelity is computed with respect to the normalized density matrices.

TABLE I. Average error measures ± standard deviation for simulated subnormalized one-qubit states for increasing simulation sampling (shots), where the distance and the fidelity are defined in the text. Results are averaged over 98 randomly generated subnormalized states prepared on the quantum device IBMQ Lagos with error mitigation.

Samples	Distance	Fidelity
2^6	0.17 ± 0.07	0.93 ± 0.06
2^8	0.09 ± 0.04	0.98 ± 0.02
2^{10}	0.06 ± 0.02	0.99 ± 0.01
2^{12}	0.06 ± 0.02	0.99 ± 0.01
2^{14}	0.06 ± 0.02	0.99 ± 0.01

Table I shows the accuracy of the state preparation for varying shot counts on the IBM Lagos device, utilizing error-mitigation techniques available in QISKIT [51]. With 2^6 samples, the fidelity is somewhat poor at 0.93; however, with only 2^{10} samples the fidelity of the prepared states has converged to be nearly exact at 0.99. The distance measure reveals the same trends in accuracy.

Preparing these subnormalized states probabilistically provides the groundwork for exploring nonunitary operations on unitary-gate-based quantum devices. Initializing the system as a superposition immediately provides the form of the diagonal unitary required to prepare the state, without needed recursive decomposition of rotation angles. Using this algorithm, we have prepared known subnormalized states which would be the result of nonunitary operations. In the next section, we demonstrate how to extend this algorithm to performing the nonunitary action of a general operator on a unitary-gate-based architecture.

B. Nonunitary evolution

The time evolution of an open quantum system can be described by the operator-sum formulation in terms of the Kraus operators,

$$\rho(t) = \sum_i \hat{K}_i \rho(0) \hat{K}_i^\dagger, \tag{14}$$

where the $\hat{K}_i$'s are the Kraus maps and $\rho(t)$ is the density matrix at time t. In general, the Kraus maps are nonunitary; however, they are always contraction mappings,

$$\sum_i \hat{K}_i \hat{K}_i^\dagger \leqslant I. \tag{15}$$

Because the Kraus operators are always contraction mappings, their singular values are always bounded above by 1, which makes Eq. (2) directly applicable without rescaling of the singular values. One can decompose each $\hat{K}_i$ using the singular-value decomposition and implement the operator as described above, as two unitaries on the original Hilbert space and a unitary diagonal on the dilated space. Each Kraus operator is simulated in parallel, and the propagated density matrix is obtained classically by Eq. (14). While we use Kraus operators in this work, the algorithm applies to any problem for which encoding the action of a nonunitary operator on a quantum state is desired and is not specific to Kraus operators.

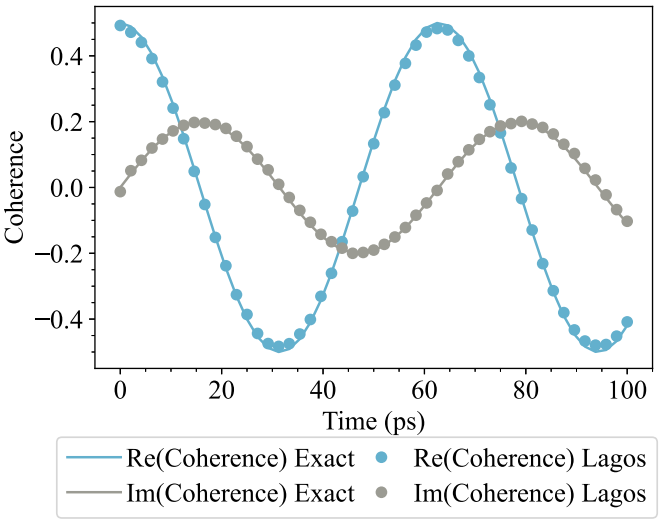

FIG. 3. Real and imaginary parts of the off-diagonal element (coherence) of a two-level state in a $Z \otimes Z$ dephasing channel. The results from the quantum device (dots) are accurate for all times in the simulation, where the exact solution (lines) is generated classically. The results from the quantum computer are generated from density-matrix tomography.

Some other examples of nonunitary operators include the Lindbladian superoperator in the unraveled Lindblad equation and (nonunitary) operators with observables.

Here, we simulate two single-qubit systems whose Kraus operators are in either diagonal or near-diagonal form, so the SVD is readily computed analytically. We used IBM's Lagos device to simulate the dynamics and performed full tomography of the system density matrix. Each simulation was performed once with the device maximum of 32 000 samples, as well as in-built error mitigation protocols, in QISKIT. We present the error-mitigated data for all results. Each circuit requires two qubits, one system qubit and one ancilla qubit.

For an initial example we simulate a two-level dephasing channel with a single qubit coupled to a one-qubit bath with a $Z \otimes Z$ interaction. This results in diagonal Kraus operators,

$$\hat{K}_0 = \sqrt{\lambda_0}\begin{pmatrix} e^{i\theta t} & 0 \\ 0 & e^{-i\theta t} \end{pmatrix}, \qquad \hat{K}_1 = \sqrt{\lambda_1}\begin{pmatrix} e^{-i\theta t} & 0 \\ 0 & e^{i\theta t} \end{pmatrix}, \tag{16}$$

where $\lambda_0 + \lambda_1 = 1$. Here, we choose the dephasing angle $\theta = 0.5\ \mathrm{ps}^{-1}$, with $\lambda_0 = 0.7$ and $\lambda_1 = 0.3$. It is clear from Eq. (16) that $\hat{K}_i/\sqrt{\lambda_i}$ is unitary and could be rescaled by λ_i classically; however, here, we simulate the nonunitary operators $\hat{K}_i$ on the device to show the nonunitary time propagation on a unitary-gate-based architecture. Figure 3 shows the time dynamics of the dephasing channel, with the exact classical solution (lines) and results from IBM Quantum (IBMQ) Lagos (circles). The initial state is chosen as $\frac{1}{\sqrt{2}}(|0\rangle + |1\rangle)$, and the populations are not time dependent, so only the coherence is shown. We performed tomography of the density matrix to generate the coherences from the quantum device, and the simulation is very accurate over the time range.

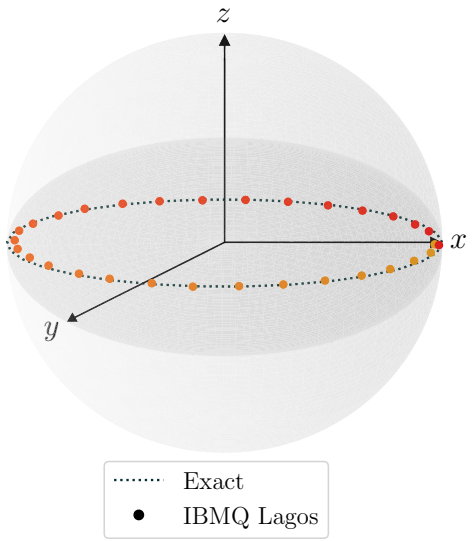

FIG. 4. The trajectory of a two-level system undergoing dephasing with a one-qubit environment is shown on a Bloch sphere with exact results represented by the dotted line and results from IBMQ Lagos represented by dots. The trajectory is in the $z = 0$ plane, represented by the dark gray circle. One period is shown (about 60 ps), where the initial state, $\frac{1}{\sqrt{2}}(|0\rangle + |1\rangle)$, is the first red dot on the right. The system explores mixed states when it is in the interior of the sphere.

Another way to visualize the time dynamics of this process is with the Bloch sphere. Because the populations are not time dependent, the state stays in the $z = 0$ plane of the Bloch sphere because of the choice of initial state. We show the Bloch sphere for the $Z \otimes Z$ dephasing process in Fig. 4. The dotted line is the exact trajectory of the state, and the dots are the simulated trajectory. Beginning in red with the initial state, we show one period of the recurring dephasing process, which is about 60 ps. The system is exploring the interior of the sphere, which indicates the system is a mixed state at those points.

For the second example, we simulate the time evolution of a two-level system in a zero-temperature amplitude damping channel. The Kraus operators in this case are

$$\hat{K}_0 = \begin{pmatrix} 1 & 0 \\ 0 & \sqrt{e^{-\gamma t}} \end{pmatrix} = I\begin{pmatrix} 1 & 0 \\ 0 & \sqrt{e^{-\gamma t}} \end{pmatrix} I, \qquad \hat{K}_1 = \begin{pmatrix} 0 & \sqrt{1-e^{-\gamma t}} \\ 0 & 0 \end{pmatrix} = I\begin{pmatrix} \sqrt{1-e^{-\gamma t}} & 0 \\ 0 & 0 \end{pmatrix} X, \tag{17}$$

where we have emphasized the form of the SVD in the last equality. Here, I is the identity, X is the Pauli X operator, and γ is the decay rate. We use $\gamma = 0.15\ \mathrm{ps}^{-1}$ for the simulations here. The chosen initial state of the system is mixed and is given by

$$\rho(0) = \frac{1}{4}\begin{pmatrix} 1 & 1 \\ 1 & 3 \end{pmatrix}. \tag{18}$$

This state can be decomposed into $|\psi_0\rangle = |1\rangle$ and $|\psi_1\rangle = \frac{1}{\sqrt{2}}(|0\rangle + |1\rangle)$, which are prepared with an X gate and H gate, respectively.

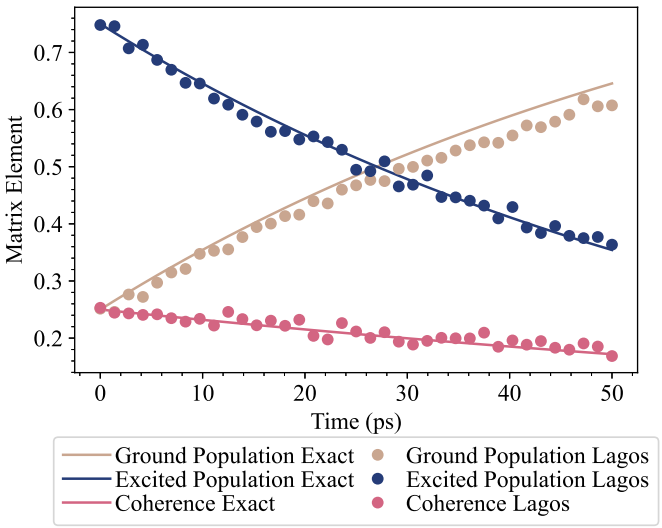

FIG. 5. Time dynamics of a zero-temperature two-level system in an amplitude-damping channel. The results from the IBMQ Lagos device (dots) are in good agreement with the exact results (solid lines). Results were generated from a single run using the device maximum of 32 000 samples (shots) with error mitigation.

The results of the simulation of the two-level amplitude-damping channel are shown in Fig. 5. The experimental results (dots) are in good agreement with the exact solution (solid lines). The populations and coherences are all modeled accurately and demonstrate the nonunitary evolution of the system as the system loses energy over time.

Description of nonunitary evolution through singular-value decomposition of the Kraus maps allows for accurate simulation of open quantum systems on unitary-gate-based quantum computers. While the SVD has a classical cost if computed numerically, in the cases presented here, the SVD of the Kraus maps is immediately available by inspection.

V. DISCUSSION

Implementation of nonunitary operations on quantum devices has important applications such as subnormalized state preparation and nonunitary dynamics. Here, we presented an algorithm based on diagonal nonunitary operators which simplifies the implementation of dense nonunitary operators. Constrained by the limited qubit number and possible gate depths in the NISQ regime, many algorithms struggle with scaling for practical implementation due to the expense of dense unitaries operating over the dilated Hilbert space.

Our algorithm implements a nonunitary operator with two unitaries on the original Hilbert space and a diagonal operator on the dilated Hilbert space. We showed that any nonunitary operator can be implemented in this way using the SVD. Assuming the classical cost of the SVD and in the limit of large system size, the circuit complexity of our algorithm is approximately half as much as a dense dilated unitary. Seen another way, our algorithm results in circuits about twice as deep compared to a unitary on the original Hilbert space.

We achieve this implementation by realizing a diagonal unitary dilation for nonunitary diagonal operators. Any nonunitary diagonal operator can be dilated to a unitary diagonal operator with only one qubit, assuming the magnitude of each element is bounded above by 1. Computing the elements of the dilated unitary is straightforward and results in an exact representation of the diagonal operator. Unitary diagonals can be exactly implemented with $2^{d+1} - 3$ one- and two-qubit gates for d qubits; however, they can also be approximately implemented with polynomial gate scaling. Future work will include exploring how approximate implementation would affect the accuracy of the overall simulation of nonunitary processes.

Our algorithm is probabilistic in that it depends on the measured state of the ancilla qubit. When the ancilla is in state $|0\rangle$, the algorithm is successful, and we have exactly prepared the state after application of a nonunitary diagonal. Future work could include implementing the algorithm with amplitude-amplification techniques, which improve the success probability of the probabilistic algorithm. This helps reduce the error from noise or reduces the number of samples required for accurate simulations.

We discussed applications of this algorithm in the context of state preparation. While our probabilistic algorithm can be used to prepare normalized states, it is better suited for the preparation of subnormalized states, which arise in the context of nonunitary state transformations. We demonstrated the preparation of one-qubit subnormalized quantum states on IBM's quantum computer Lagos with high accuracy and fidelity using our algorithm and showed the states can be prepared accurately with a relatively modest number of samples or shots.

We also applied our algorithm to two time-dependent open quantum systems, which undergo nonunitary evolution. Using the SVD, we showed that any nonunitary operator can be decomposed and implemented with one ancilla qubit using the unitary diagonal construction for the singular values. We used the SVD to decompose the Kraus operators for the dynamics; however, the algorithm is applicable to any operator. We accurately reproduced the nonunitary dynamics of a two-level dephasing channel and a two-level amplitude damping channel using IBM's Lagos quantum computer. Our algorithm is particularly useful when the cost of the SVD is not prohibitive, which is the case for most operators considered in the NISQ era. Furthermore, because the diagonal unitary dilation is exact, we can implement the entire nonunitary process on one quantum circuit, which is useful when further transformation of the state is desired.

Our algorithm is effective in implementing nonunitary operations in quantum simulation in the NISQ era. Beyond state preparation and nonunitary dynamics, our algorithm will also be useful in computing expectation values of nonunitary observables without controlled unitaries in the Hadamard test. Quantum-classical hybrid methods may also benefit from our algorithm when the SVD of the relevant operators can be computed. Moreover, future work may be able to exploit operator structure and symmetries to decrease the computational cost of the classical decomposition, facilitating the application of our algorithm to larger systems of interest. Our algorithm provides an intuitive look at the action of nonunitary operators in the qubit space and reduces the dilation problem to the implementation of a dilated diagonal unitary based on the singular values of an operator.

ACKNOWLEDGMENTS

This work is supported by the NSF RAISE-QAC-QSA, Grant No. DMR-2037783, and the Department of Energy, Office of Basic Energy Sciences, Grant No. DE-SC0019215. D.A.M. also acknowledges NSF EAGER-QAC-QSA, Grant No. CHE-2035876. We acknowledge the use of IBM Quantum services for this work. The views expressed are those of the authors and do not reflect the official policy or position of IBM or the IBM Quantum team.

[1] J. Preskill, Quantum computing in the NISQ era and beyond, Quantum **2**, 79 (2018).

[2] S. Kais, in *Quantum Information and Computation for Chemistry* (Wiley, Hoboken, NJ, 2014)

[3] Y. Cao, J. Romero, J. P. Olson, M. Degroote, P. D. Johnson, M. Kieferová, I. D. Kivlichan, T. Menke, B. Peropadre, N. P. D. Sawaya, S. Sim, L. Veis, and A. Aspuru-Guzik, Quantum chemistry in the age of quantum computing, Chem. Rev. **119**, 10856 (2019).

[4] K. Head-Marsden, J. Flick, C. J. Ciccarino, and P. Narang, Quantum information and algorithms for correlated quantum matter, Chem. Rev. **121**, 3061 (2021).

[5] S. McArdle, S. Endo, A. Aspuru-Guzik, S. C. Benjamin, and X. Yuan, Quantum computational chemistry, Rev. Mod. Phys. **92**, 015003 (2020).

[6] M. Motta and J. E. Rice, Emerging quantum computing algorithms for quantum chemistry, WIREs Comput. Mol. Sci. **12**, e1580 (2022).

[7] K. Bharti, A. Cervera-Lierta, T. H. Kyaw, T. Haug, S. Alperin-Lea, A. Anand, M. Degroote, H. Heimonen, J. S. Kottmann, T. Menke, W.-K. Mok, S. Sim, L.-C. Kwek, and A. Aspuru-Guzik, Noisy intermediate-scale quantum algorithms, Rev. Mod. Phys. **94**, 015004 (2022).

[8] R. Sweke, I. Sinayskiy, and F. Petruccione, Simulation of single-qubit open quantum systems, Phys. Rev. A **90**, 022331 (2014).

[9] R. Sweke, I. Sinayskiy, D. Bernard, and F. Petruccione, Universal simulation of Markovian open quantum systems, Phys. Rev. A **91**, 062308 (2015).

[10] Z. Hu, R. Xia, and S. Kais, A quantum algorithm for evolving open quantum dynamics on quantum computing devices, Sci. Rep. **10**, 3301 (2020).

[11] K. Head-Marsden, S. Krastanov, D. A. Mazziotti, and P. Narang, Capturing non-Markovian dynamics on near-term quantum computers, Phys. Rev. Research **3**, 013182 (2021).

[12] Z. Hu, K. Head-Marsden, D. A. Mazziotti, P. Narang, and S. Kais, A general quantum algorithm for open quantum dynamics demonstrated with the Fenna-Matthews-Olson complex, Quantum **6**, 726 (2022).

[13] A. Gaikwad, Arvind, and K. Dorai, Simulating open quantum dynamics on an NMR quantum processor using the Sz.-Nagy dilation algorithm, arXiv:2201.07687.

[14] A. W. Schlimgen, K. Head-Marsden, L. M. Sager, P. Narang, and D. A. Mazziotti, Quantum Simulation of Open Quantum Systems Using a Unitary Decomposition of Operators, Phys. Rev. Lett. **127**, 270503 (2021).

[15] A. W. Schlimgen, K. Head-Marsden, L. M. Sager, P. Narang, and D. A. Mazziotti, Quantum simulation of the Lindblad equation using a unitary decomposition of operators, Phys. Rev. Research **4**, 023216 (2022).

[16] H. Kamakari, S.-N. Sun, M. Motta, and A. J. Minnich, Digital quantum simulation of open quantum systems using quantum imaginary–time evolution, PRX Quantum **3**, 010320 (2022).

[17] S.-J. Wei, D. Ruan, and G.-L. Long, Duality quantum algorithm efficiently simulates open quantum systems, Sci. Rep. **6**, 30727 (2016).

[18] C. Zheng, Universal quantum simulation of single-qubit nonunitary operators using duality quantum algorithm, Sci. Rep. **11**, 3960 (2021).

[19] S. Endo, J. Sun, Y. Li, S. C. Benjamin, and X. Yuan, Variational Quantum Simulation of General Processes, Phys. Rev. Lett. **125**, 010501 (2020).

[20] M. Cattaneo, M. A. C. Rossi, G. García-Pérez, R. Zambrini, and S. Maniscalco, Quantum simulation of dissipative collective effects on noisy quantum computers, arXiv:2201.11597.

[21] C. W. Kim, J. M. Nichol, A. N. Jordan, and I. Franco, Analog quantum simulation of the dynamics of open quantum systems, arXiv:2203.12127.

[22] R. Sweke, M. Sanz, I. Sinayskiy, F. Petruccione, and E. Solano, Digital quantum simulation of many-body non-Markovian dynamics, Phys. Rev. A **94**, 022317 (2016).

[23] A. Chenu, M. Beau, J. Cao, and A. del Campo, Quantum Simulation of Generic Many-Body Open System Dynamics Using Classical Noise, Phys. Rev. Lett. **118**, 140403 (2017).

[24] H.-Y. Su and Y. Li, Quantum algorithm for the simulation of open-system dynamics and thermalization, Phys. Rev. A **101**, 012328 (2020).

[25] S. Patsch, S. Maniscalco, and C. P. Koch, Simulation of open-quantum-system dynamics using the quantum Zeno effect, Phys. Rev. Research **2**, 023133 (2020).

[26] G. Garcia-Perez, M. A. C. Rossi, and S. Maniscalco, IBM Q Experience as a versatile experimental testbed for simulating open quantum systems, npj Quantum Inf. **6**, 1 (2020).

[27] B. Rost, B. Jones, M. Vyushkova, A. Ali, C. Cullip, A. Vyushkov, and J. Nabrzyski, Simulation of thermal relaxation in spin chemistry systems on a quantum computer using inherent qubit decoherence, arXiv:2001.00794.

[28] B. Rost, L. Del Re, N. Earnest, A. F. Kemper, B. Jones, and J. K. Freericks, Demonstrating robust simulation of driven-dissipative problems on near-term quantum computers, arXiv:2108.01183.

[29] M. Metcalf, E. Stone, K. Klymko, A. F. Kemper, M. Sarovar, and W. A. de Jong, Quantum Markov chain Monte Carlo with digital dissipative dynamics on quantum computers, Quantum Sci. Technol. **7**, 025017 (2022).

[30] J. D. Guimarães, M. I. Vasilevskiy, and L. S. Barbosa, Efficient method to simulate non-perturbative dynamics of an open quantum system using a quantum computer, arXiv:2203.14653.

[31] T. Xin, S.-J. Wei, J. S. Pedernales, E. Solano, and G.-L. Long, Quantum simulation of quantum channels in nuclear magnetic resonance, Phys. Rev. A **96**, 062303 (2017).

[32] A. M. Childs and T. Li, Efficient simulation of sparse Markovian quantum dynamics, Quantum Inf. Comput. **17**, 0901 (2017).

[33] R. Cleve and C. Wang, Efficient quantum algorithms for simulating Lindblad evolution, arXiv:1612.09512.

[34] J. Welch, D. Greenbaum, S. Mostame, and A. Aspuru-Guzik, Efficient quantum circuits for diagonal unitaries without ancillas, New J. Phys. **16**, 033040 (2014).

[35] V. Shende, S. Bullock, and I. Markov, Synthesis of quantum-logic circuits, IEEE Trans. Comput.-Aided Des. Integr. Circuits Syst. **25**, 1000 (2006).

[36] G. Brassard, P. Høyer, M. Mosca, and A. Tapp, Quantum amplitude amplification and estimation, *Quantum Computation and Information* (American Mathematical Society, Providence, RI, 2002), pp. 53–74.

[37] K. Nakaji, Faster amplitude estimation, Quantum Inf. Comput. **20**, 1109 (2020).

[38] Y. Suzuki, S. Uno, R. Raymond, T. Tanaka, T. Onodera, and N. Yamamoto, Amplitude estimation without phase estimation, Quantum Inf. Process. **19**, 75 (2020).

[39] D. Grinko, J. Gacon, C. Zoufal, and S. Woerner, Iterative quantum amplitude estimation, npj Quantum Inf. **7**, 52 (2021).

[40] W. F. Stinespring, Positive functions on c*-algebras, Proc. Am. Math. Soc. **6**, 211 (1955).

[41] F. Buscemi, G. M. D'Ariano, and M. F. Sacchi, Physical realizations of quantum operations, Phys. Rev. A **68**, 042113 (2003).

[42] M. A. Nielsen and I. L. Chuang, *Quantum Computation and Quantum Information*, 10th anniversary ed. (Cambridge University Press, Cambridge, 2010).

[43] C. P. Williams, Probabilistic nonunitary quantum computing, SPIE Proc. 5436, 297 (2004).

[44] T. Liu, J.-G. Liu, and H. Fan, Probabilistic nonunitary gate in imaginary time evolution, Quantum Inf. Process. **20**, 204 (2021).

[45] T. Xin, S. Wei, J. Cui, J. Xiao, I. Arrazola, L. Lamata, X. Kong, D. Lu, E. Solano, and G. Long, Quantum algorithm for solving linear differential equations: Theory and experiment, Phys. Rev. A **101**, 032307 (2020).

[46] D. W. Berry, A. M. Childs, R. Cleve, R. Kothari, and R. D. Somma, Exponential improvement in precision for simulating sparse Hamiltonians, in *Proceedings of the Forty-Sixth Annual ACM Symposium on Theory of Computing, STOC '14* (Association for Computing Machinery, New York, 2014), pp. 283–292.

[47] A. M. Childs and N. Wiebe, Hamiltonian simulation using linear combinations of unitary operations, Quantum Inf. Comput. **12**, 901 (2012).

[48] S. S. Bullock and I. L. Markov, Asymptotically optimal circuits for arbitrary n-qubit diagonal computations, Quantum Inf. Comput. **4**, 27 (2004).

[49] S. Lloyd, Universal quantum simulators, Science **273**, 1073 (1996).

[50] H. Abraham *et al.*, QISKIT, an open-source framework for quantum computing, 2019, doi:10.5281/zenodo.2562110.

[51] IBM-Q-Team, IBM-Q-7 Lagos backend specification v1.0.27 (2022), https://quantum-computing.ibm.com/.